Synthesis and Characterization Some Complexes of Mixed Ligand and Study Its Effects as Antioxidant and Anticancer

Mieaad Mohammed Reda[*] and Layla Ali Mohammed[**]

[*]Department. of Chemistry, College of science, University of Kufa,
[**]Department. of Chemistry, College of Education for Girls, University of Kufa.

E-mail: miaadm.hassan@uokufa.edu.iq , **E-mail: Laila.alameri@uokufa.edu.iq

Abstract:
A series of mixed ligand complexes of Co(II), Ni(II), Cu(II), Zn (II),Cd(II), Fe (III) and Au(III) were prepared and characterized. A new azo ligand derived from 4-methylimidazole with sulfadiazine and Schiff base derived from 4-(dimethylamino)-2-hydroxobenzaldehyde and 4-amino-3-hydroxy benzene sulfonamide. Ligands structures and their transitional metal mix-ligand complexes were characterized using various analytical techniques, including molar conductance, elemental analysis (C.H.N), electronic spectral, magnetic measurements, ^{1}HNMR, IR spectral studies and mass spectra. The data shows that these complexes have composition of $[ML_1L_2H_2O]$ where M = Co(II), Ni(II), Cu(II), Zn(II) ,Cd(II) and Hg(II). $[ML_1L_2Cl]$ where M=Fe(III). $[ML_1L_2]Cl_2$ where M=Au(III). The magnetic susceptibility and electronic spectral data of the complexes indicate that the octahedral geometry of all complexes, except the complex of Au(III) indicates a square plane geometry. The IR results demonstrate that the co-ordination sites are imidazole nitrogen atom and the farthest azo nitrogen atom of L_1 as natural bidentate with nitrogen the azomethine and oxygen atoms of Schiff base L_4. Azo ligand and Schiff base behave as tridentate manner. All the compounds showed DPPH radical scavenging activity. In general, the results indicated that the complexes have potential and promising anti-oxidant activities.

Keywords: new mixed ligand complexes, azo and Schiff base ligands ,antioxidants, anticancrer .

1. Introduction

Schiff bases, are more versatile compounds in coordination chemistry, as they have many significant biological applications including antifungal, antibacterial, antiviral, anticancer and antioxidant activities [1–8]. In addition, role of Schiff bases and their complexes in

catalytic reactions such as oxidation, reduction, hydrolysis reactions, inhibition of corrosion and memory storage devices in electronics are also reported [9–12]. Over the years, mixed-ligand complexes have been attraction in worldwide due to their several biological, enzymatic and analytical applications [13].

Azo - derivative Imidazole ligands have attracted the attention of many researches working in the field of coordination chemistry. This type of ligands that contain the azo imine group(-N=N-C=N-), that give feature high stability to metallic complexes due to the back bonding.

Therefore, it has a wide range of applications in all fields, as it has shown its medical efficiency in the treatment of prostate and breast cancer [14,15], as it had a pharmacological effect in inhibiting cancer cells.

In the scientific filed, it has proven its great effectiveness in analytical chemistry in separation, isolating and diagnosing metal ions by extracting them from different environmental and biological samples [16,17]

2. Experimental and Materials

All chemicals were supplied by BHD and Sigma Aldrich, and A.K.Scie , Fluka and used without further purification .,The electro-thermal melting point model 9300 was used to measure the melting point of the ligand and its complexes. Elemental analyses were carried out by means of micro analytical unit of 1180 C.H.N elemental analyzer. Electronic spectra were recorded on Shimadzu spectrophotometer double beam model 1700 ultraviolet-visible (UV-Vis) spectrophotometer. . Fourier-transform infrared (FTIR) spectra were recorded in KBr disc on FTIR Shimadzu spectrophotometer model 8400 in wave number 4000- 400/cm. Proton nuclear magnetic resonance (1H-NMR) and carbon nuclear magnetic resonance (13C-NMR) spectra in ppm unit were operating in dimethyl sulfoxide-d6 (DMSO-d6) as solvent using (Bruker) Ultra Shield 3000 MHz, Switzerland). And mass spectra were recorded on AB Sciex 3200 QTRAP LC/ MS/MS (mass range m/z 5- 2000 quad mode and 50- 1700 linear ion trap mode). Magnetic susceptibility measurements were carried out on a balance magnetic MSB-MKI using faraday method. The diamagnetic corrections were made by Pascal's constants.

2.1 preparation of Azo Ligand

This heterocyclic azo ligand was prepared as described before [18] (Scheme.1). A solution of 4-amino N-(Pyrimidin-2-yl)benzenesulfonamide) (2.47 g,0.01mol) in (100 mL) water and (3 mL) concentrated HCl (37%) was whiskered until a clear solution was get. Where, this solution is cooled to (0–5 ^{O}C) and while maintaining the temperature below (5 ^{O}C) a solution of sodium nitrite (0.72 g, 0.01mol) in 10 mL water was then

added drop by drop. The resulting mixture was stirred for (30 min) in an ice bath and the excess nitrite was removed with the addition of urea [19]. The solution of resulting diazonium chloride was mixed with coupling component 4- methyl-1H-imidazole (0.82 g, 0.01 mol) dissolved in (150 mL) from cooled alkaline ethanol under (5 ^{O}C). After the solution was left in the refrigerator for 24 hours, the mixture was acidified with hydrochloric acid diluted to (pH = 6). The red precipitate was washed and filtered several times by using distilled water, then dried in air and twice re-crystallized with hot ethanol, then it was dried using the oven at (50 ^{O}C). Some analytical and physical data for this azo dye was tabulated in Table (1) Scheme 1 shows the preparation steps of the azo ligand

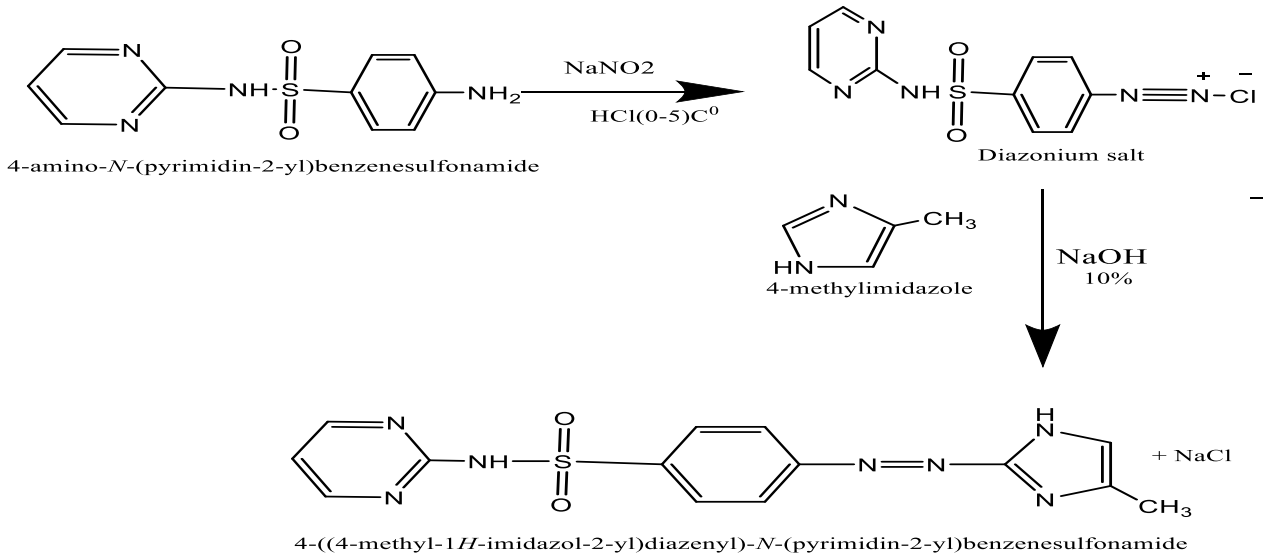

Scheme 1: Preparation of azo Ligand (L_1)

2.2 Preparation of the Schiff base (HL_2):

(0.149.19 g ,0.01 mol) from (4-dimethylamino)benzaldehyde dissolved in ethanol (50 mL) and then mixed with (o.188 g ,0.01mol) of (4-amino3-hydroxobenzenesulfonamide) dissolved in ethanol. Three drops from glacial acetic acid ware added and the mixture was refluxed with stirring for 6 hrs. Schiff base ligand was isolated after the volume of the mixture was reduced to half by evaporation and precipitated product was collected by filtered off and dried over anhydrous $CaCl_2$. Yield:96%, mp:(198-200) ^{0} C. Scheme 2 show the preparation steps of the Schiff base ligand

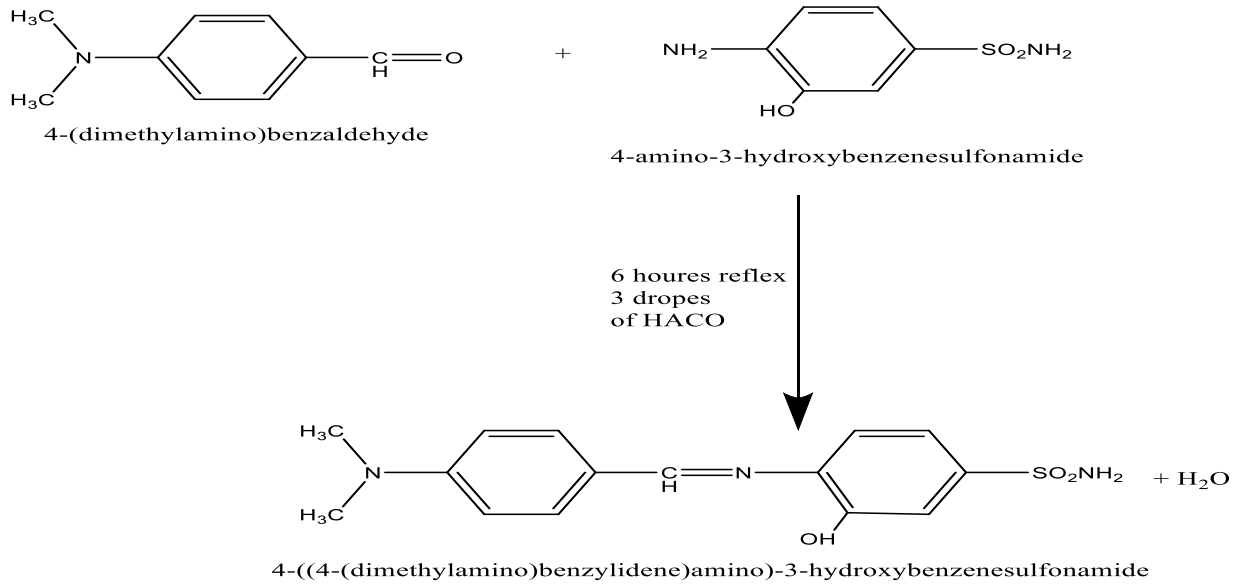

Scheme 2: preparation Ligand Schiff base (HL_2)

2.3 Preparation complex of Mixed ligand L_1 and HL_2:

General procedure for preparation chelate complexes, the alcohol solution of respective salts [$NiCl_2.6H_2O$, $CoCl_2.6H_2O$, $CuCl_2.2H_2O$, $ZnCl_2$,$Cdcl_2$, $HgCl_2$ and $Na[AuCl_4].2H_2O$] was slowly mixed with hot mixture ethanolic solution of **(L_1)** and (HL_2) ligand, in (1:1:1) (L: M: L) molar ratio. After the addition was complete, the reaction mixture was refluxed for (2 houres) then cooled. The solids that precipitate were filtered off, washed with (5 mL) hot (50%) (ethanol:water) to take out any effects of the unreacted starting materials, air dried, re-crystallized from ethanol and heated in the oven at (60 ^{O}C). All data for these compounds tabulated in Table (1).

2.4. Antioxidant activity

The free radical scavenging activity of the synthesized compounds was studied in vitro by 1, 1-diphenyl-2-picrylhydrazyl (DPPH) assay method.[20] Stock solution of the drug was diluted to different concentrations in the range of 50-200 mg/ mL in methanol. Methanolic solution of the synthesized compounds (2 mL) was added to 0.003% (w/v) methanol solution of DPPH (1 mL). The mixture was shaken vigorously and allowed to stand for 30 min. Absorbance at 517 nm was determined and the percentage of scavenging activity was calculated. Ascorbic acid was used as the standard drug. The inhibition ratio (I %) of the tested compounds was calculated according to the following equation: I % = (Ac-As)/Ac X 100, where Ac is the absorbance of the control and As is the absorbance of the sample.

3. Results and Discussion

All mixed ligand complexes in this research were Freely dissolvable by DMF, DMSO, Ethanol and Methanol. Also, they were stable in air. The complexes of metal were characterized by molar conductivities, elemental analysis, magnetic susceptibility, UV-Vis, IR, mass spectra and ^{1}H,MNR spectra. The results of analysis for the complexes were a good agreement with the results of experiment. The value display that the (metal: ligand) ratio is (1:1:1) and are shown in table 1. At room temperature, the magnetic susceptibility of the chelate complexes were a good agreement with octahedral molecular geometry, except the complex of Au(III) indicates a Square planar molecular geometry about the central ion of metal. Most of prepared chelate complexes in this research was exhibited lower conductivity values of the complexes. This is evidence that complexes have non-electrolytic nature. Except the complex of Au(III) which exhibited higher conduction values supporting the electrolytic nature of the metal complexes.

3.1.Micro-element analysis

In table (1), the results of micro-element analysis for ratio complexes 1:1:1 [L:M:L] exhibited that the results of theoretical were a good agreement with the found results. C,H,N elemental analysis and TLC technique were used to test the purity of mixed ligand.

Table 1. Some Physical properties and -elemental micro analysis

Compound	Chemical formula	M.P(C°)	Yield %	Color	C Found % (cal.)	H Found % (cal.)	N Found % (cal.)
Ligand=L_1	$C_{14}H_{13}N_7O_2S$	177-180	82	Brown	48.93 (48.95)	3.76 (3.78)	28.63 (28.55)
Ligand=HL_2	$C_{15}H_{17}N_3O_3S$	198-200	96	Orange	53.62 (53.67)	5.02 (5.06)	12.49 (12.52)
$[Co(L_1L_2)H_2OCl]$	$CoC_{29}H_{31}N_{10}O_6S_2Cl$	175-177	80	Brown	46.14 (46.22)	3.73 (3.98)	18.47 (18.59)
$[Ni(L_1L_2)H_2OCl]$	$NiC_{29}H_{31}N_{10}O_6S_2Cl$	310 Dec.	83	Dark red	46.11 (46.23)	3.68 (3.96)	18.36 (18.59)
$[Cu(L_1L_2)H_2OCl]$	$CuC_{29}H_{31}N_{10}O_6S_2Cl$	223-225	84	Dark brown	45.79 (45.94)	3.72 (3.96)	18.29 (18.48)
$[Zn(L_1L_2)H_2OCl]$	$ZnC_{29}H_{31}N_{10}O_6S_2Cl$	248-250	74	Red	45.59 (45.82)	3.69 (3.95)	18.25 (18.43)
$[Cd(L_1L_2)H_2OCl]$	$CdC_{29}H_{31}N_{10}O_6S_2Cl$	173-175	79	Dark red	43.06 (43.17)	3.50 (3.72)	16.98 (17.36)
$[Hg(L_1L_2)H_2OCl]$	$HgC_{29}H_{31}N_{10}O_6S_2Cl$	250-253	82	Red	38.77 (38.90)	3.19 (3.35)	15.47 (15.65)
$[Fe(L_1L_2)Cl_2]$	$FeC_{29}H_{29}N_{10}O_5S_2Cl_2$	310 Dec.	86	Dark green	45.18 (45.35)	3.48 (3.64)	17.95 (18.24)
$[Au(L_1L_2)]Cl_2$	$AuC_{29}H_{29}N_{10}O_5S_2Cl_2$	222-225	77	Red	36.62 (36.86)	2.72 (2.96)	14.68 (14.83)

3.2. Mass spectra

At room temperature, the mass spectra of synthesis of Ligands were recorded. The proposed formula of the synthesized compounds was confirmed using the obtained molecular ion peaks. The mass spectra of Azo Ligand (L_1) showed the peak of molecular ion at m/z^+ 343.2 (3.28%) compound ($C_{14}H_{13}N_7O_2S$) and this confirms the proposed formula of the synthesized compounds. As well as, the mass spectra of the Schiff base (HL_2) showed the peak of molecular ion at m/z^+ 335 (5.42%) compound ($C_{15}H_{17}N_3O_4S$) and this confirms the proposed formula of the synthesized compounds.

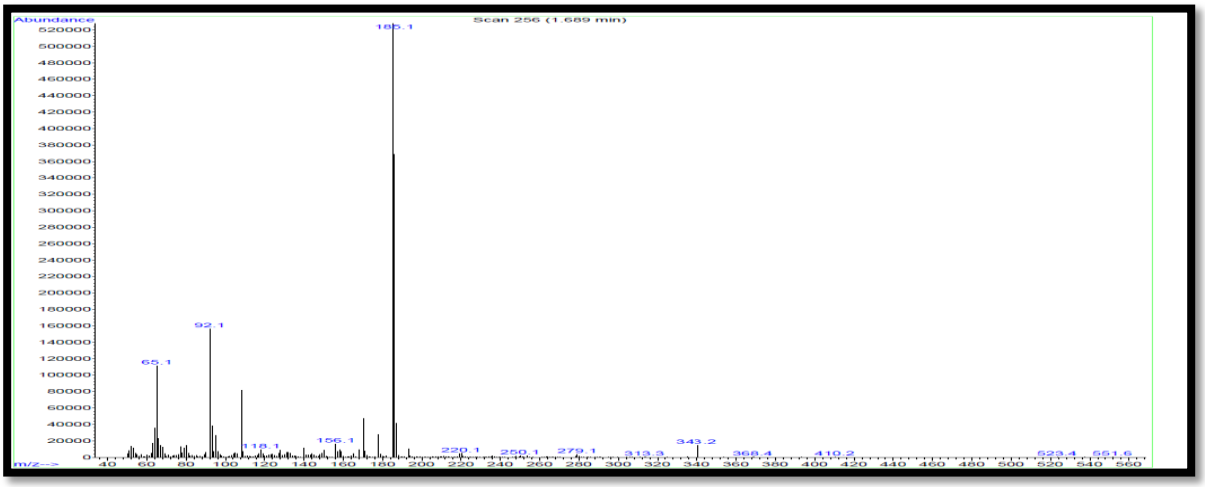

(a)

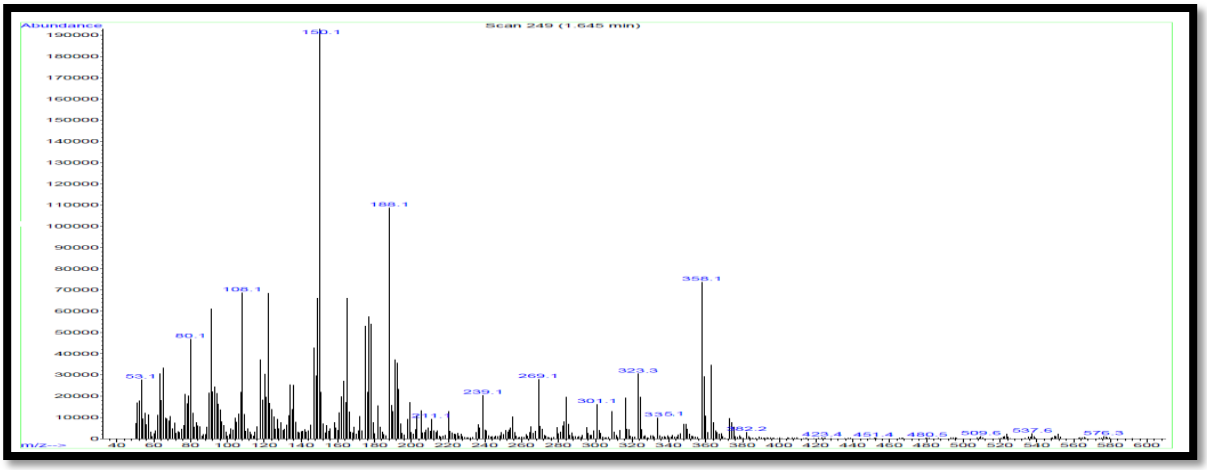

(b)

Figure (1) : (a) Mass spectra of the azo-ligand (L_1) ,(b) Mass spectra of the Schiff base ligand (HL_2)

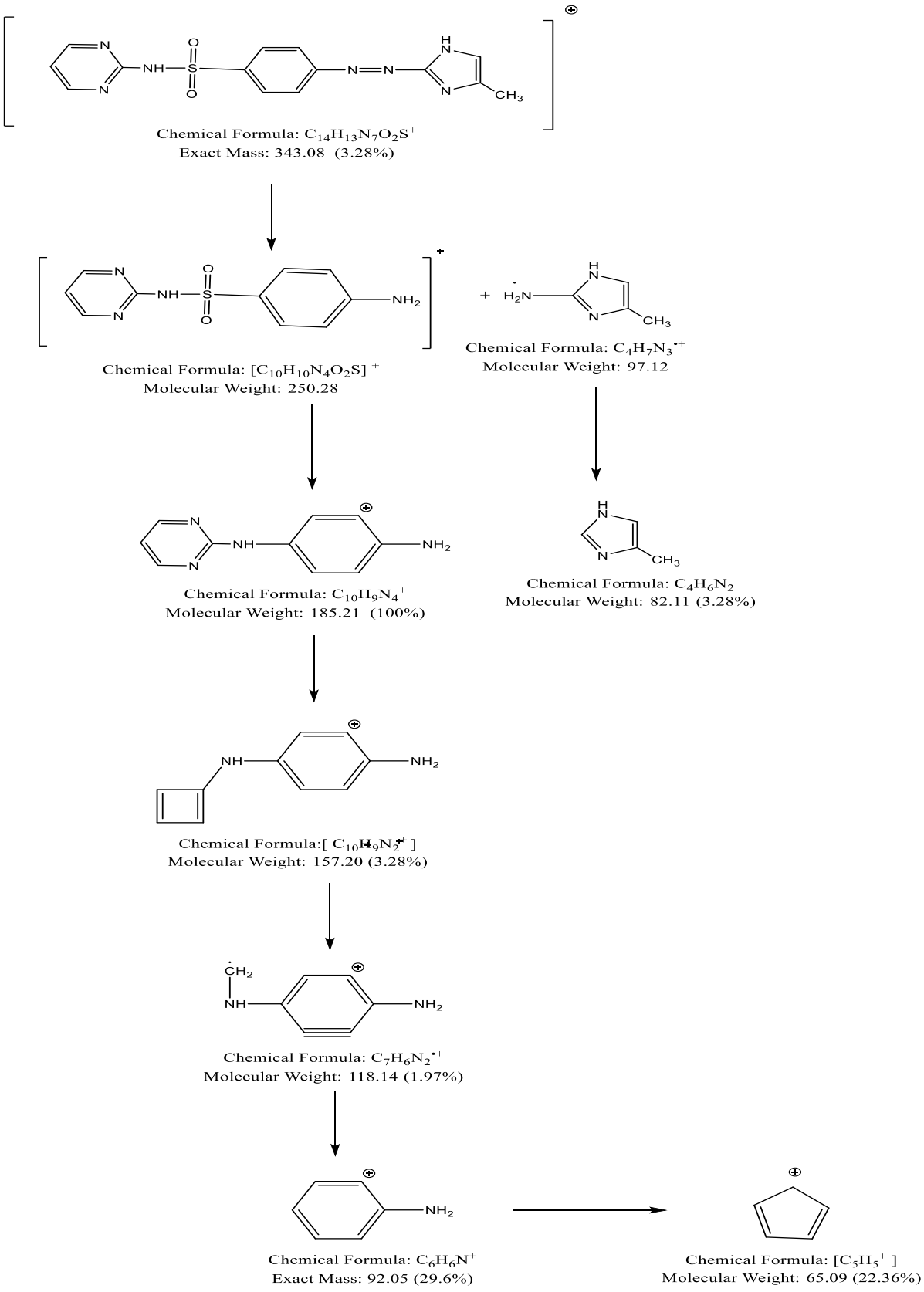

Scheme 2 : Fragment of Azo ligand (L_1)

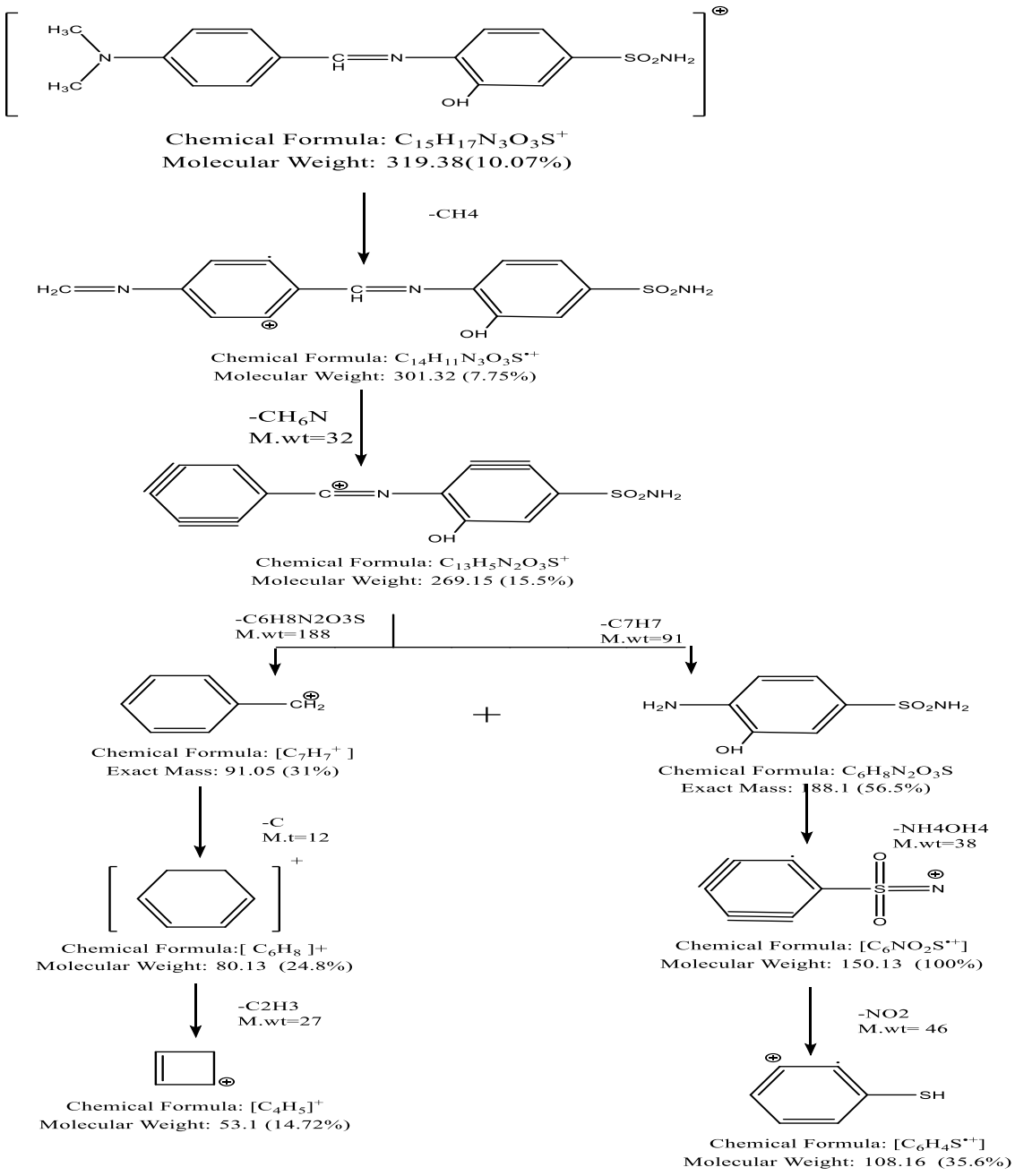

Scheme 3 : Fragment of Schiff base ligand (HL_2)

3.3.1 ^{1}HNMR Spectrum of azo- ligand L_1

^{1}HNMR spectrum of this compound was recorded by DMSO-d6. The singlet signal at δ 2.5 ppm was due to the methoxy protons. The aromatic protons were seen in the range of δ 6.5 –8.5 ppm as multiple signals. CH_3 imidazole ring at 1.2 ppm, another signal at δ 13.0 ppm attributed to imidazole (-NH-) proton and singlet at δ 4.3 ppm due to (NH-) sulfadiazine [21-23]

3.3.2.^{1}HNMR Spectrum of Schiff base- ligand HL_2

The assignment of the main signal in the ^{1}HNMR spectra of Schiff-base ligand showed a signal at δ 4.9 ppm was due to group (-NH_2) of sulfonamide ring. The aromatic protons were seen in the range of δ 6.04 –7.69 ppm as multiple signals. the singlet single at δ 8.6 ppm belong to proton (CH=N) of Schiff group, also signals at δ 10.4 ppm attributed to group (OH) and at δ 13.7 ppm belong to proton group (NH) related to sulfonamide ring which forming hydrogen bonding with nitrogen of (CH=N-), while a signal at δ 2.5 ppm returned to the solvent.

the complex (Cd) of mixed ligand show nearly the same signals which belong to L_1,HL_2 except disappear signal attributed to proton of (OH) since it contributed to coordination as the complex new signal at (δ 3.3) ppm refers to protons of water molecule inside coordination sphere.

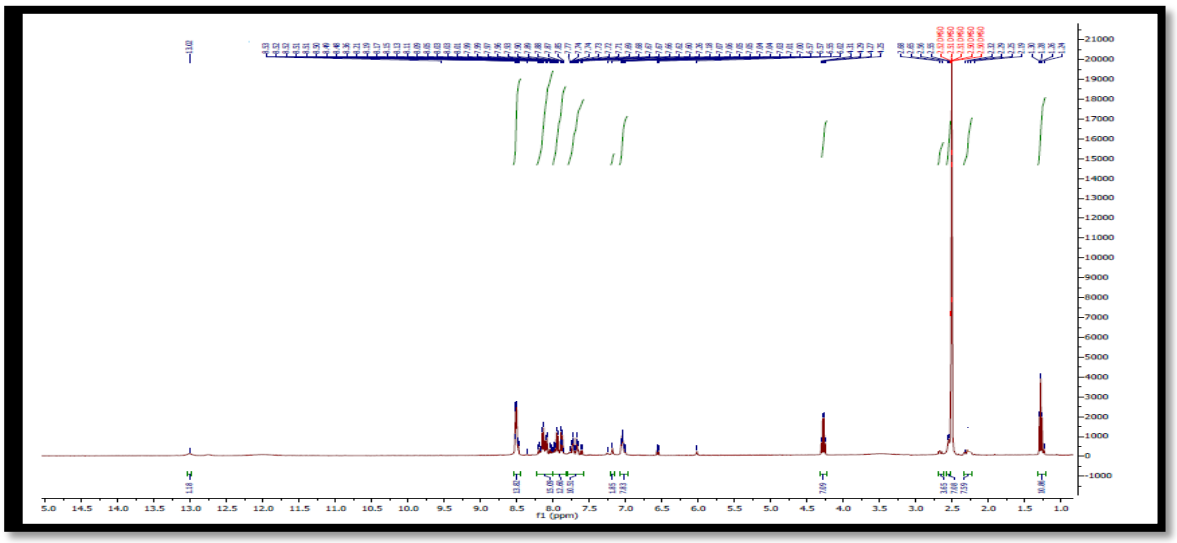

(a)

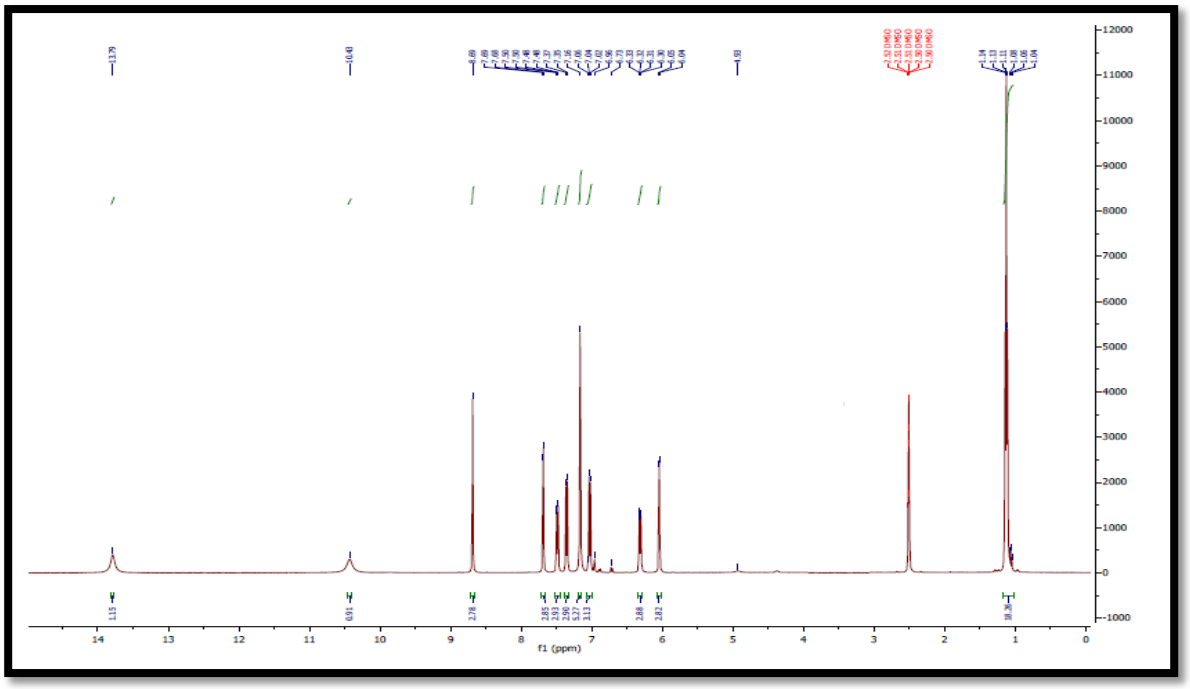

(b)

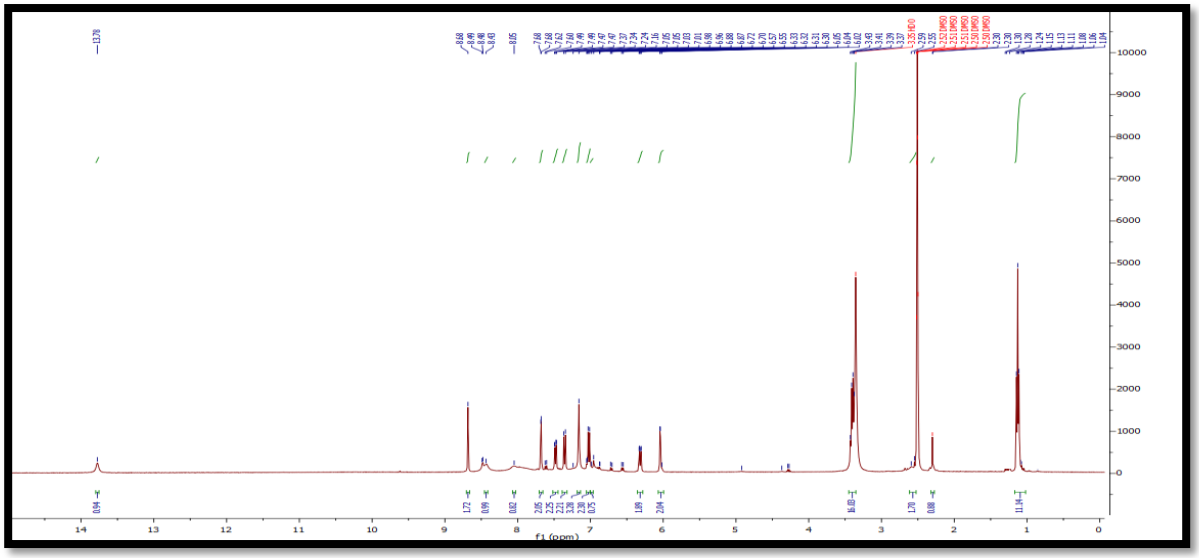

(c)

Figure (2) The ^{1}HNMR spectrum of ligand (a) (L_1) and (b) (HL_2(c) Cd complex of Mixed ligand

4. Infrared spectra

The IR spectra of the complexes are compared with that of the free ligands to determine the changes that might have taken place during the complexion, all data are listed in table (2).

The bands assigned to the azomethine group (C=N) in the Schiff base ligands (HL_2) were observed at (1602) cm^{-1} and shifted to lower frequency in all metal complexes. This indicates the participation of the nitrogen atom of the azomethine group in coordination [24]. Abroad vibration bands at (3419) cm^{-1} in the ligand (HL_2) were assigned to the phenolic OH group. The dis appearance of this peak in the spectra of all the complexes indicates the de protonation of phenol proton prior to coordination, the bands which appear in refers to water molecule inside coordination sphere. Also, the azo ligand L_1 exhibits a band at (1446) cm^{-1} assignable to (N=N) group and shifted to lower frequency in metal complexes this indicates the participation of the nitrogen atom of the azo group in coordination [25,26].The presence of coordinated water molecules in complexes ware observed by broad bonds around (3361-3415) cm^{-1} except the complex of Au(III) and Fe(III).The spectrum of free ligand (L_2) show two absorption bands at (1346) cm^{-1} and (1143) cm^{-1} due to symmetrical and asymmetrical vibration of (O=S=O) group[27-28], these bands are stable in position and intensity in free ligand and its metal complexes. The IR spectra of all complexes showed new bands at about (576-590) and (445-462)cm^{-1} assigned to υ (M-N), υ (M-O)respectively. Representative example for their spectra is given in Fig(3).

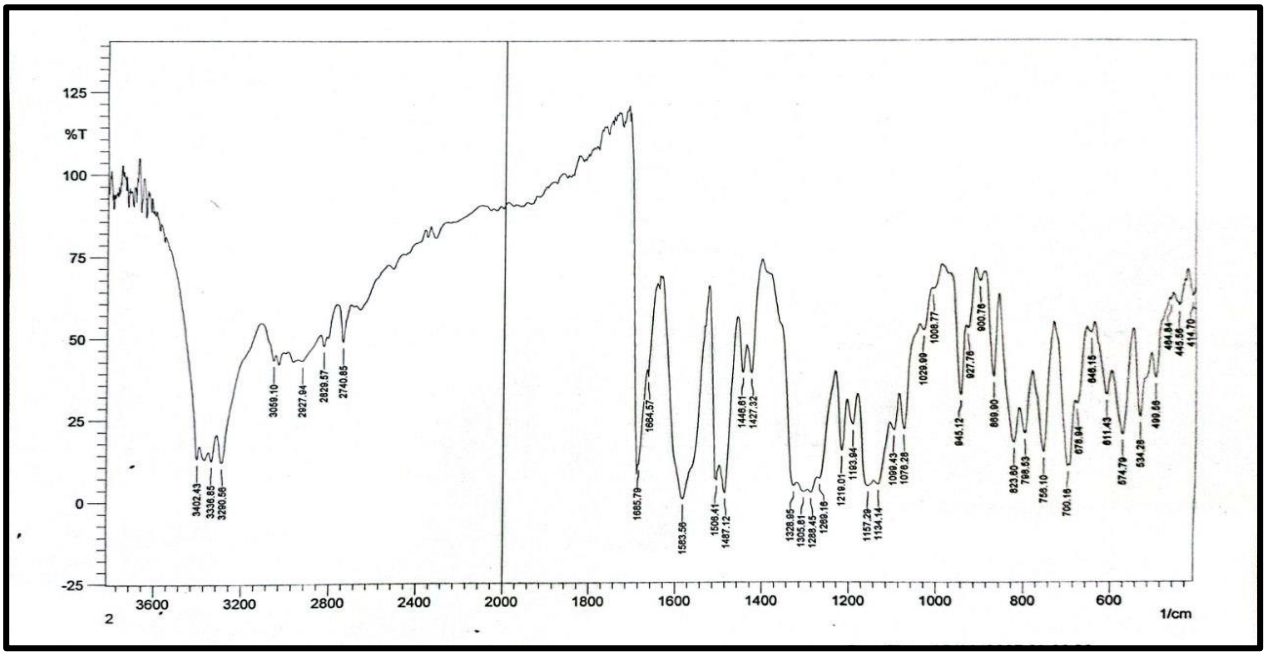

(a)

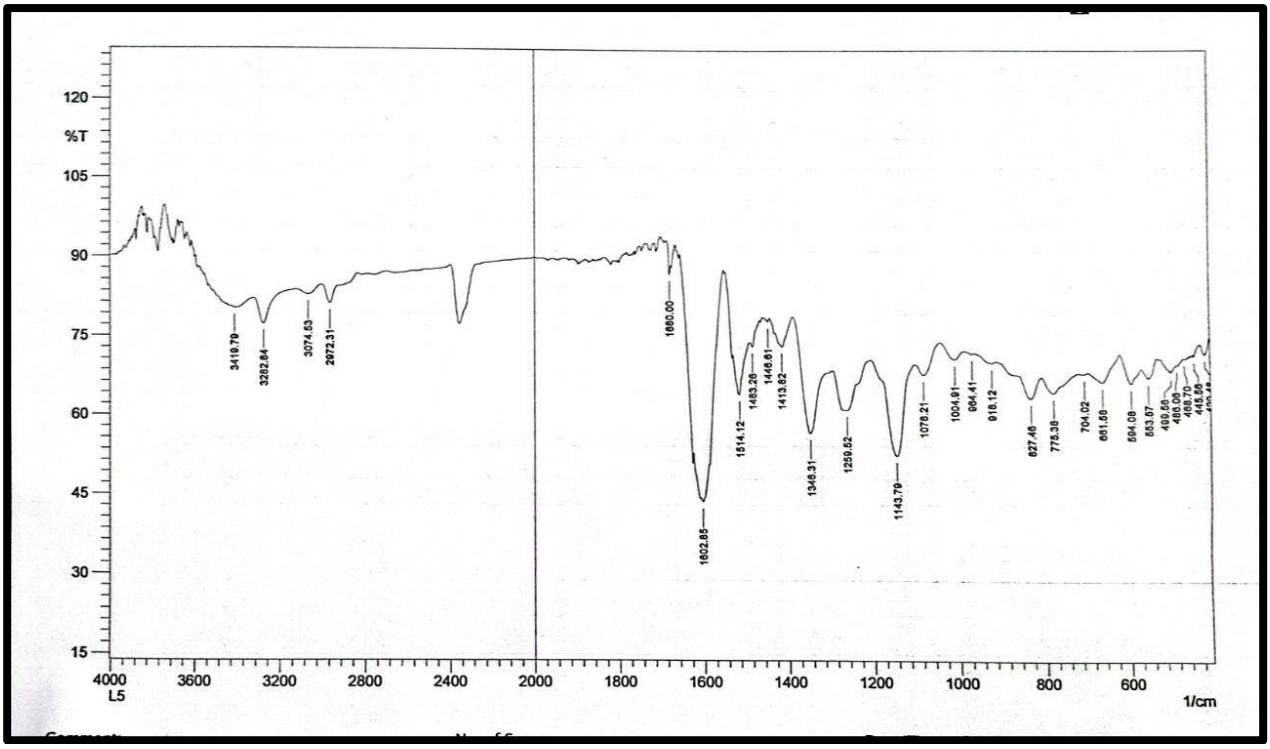

(b)

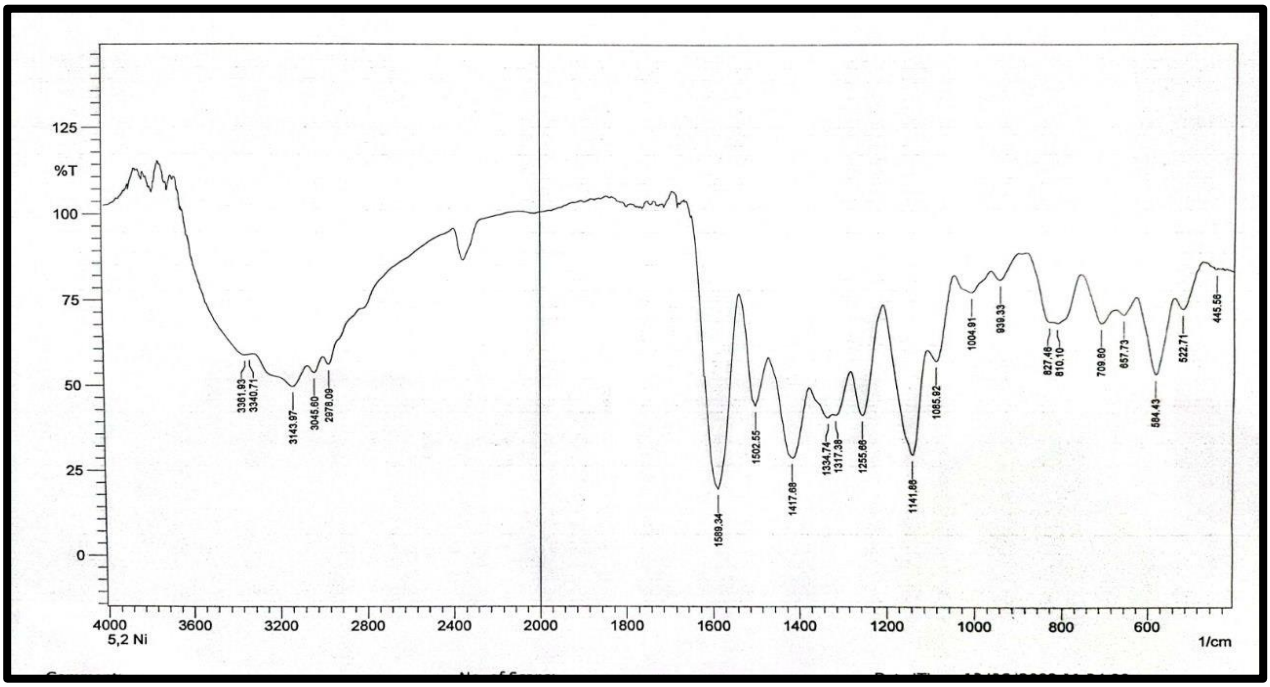

(c)

Figure (3): IR- spectrum of (a) azo ligand L_1, (b) Schiff base ligand HL_2, (C) complex of mixed ligand [$[NiL_1L_2H_2OCl]$

Table 2: Characteristic IR frequencies of the ligand (L_1) and (HL_2) and Mixed ligand Complexes

Compound	υ(O-H) H_2O	υ(C=N) Schiff	υ(N=N)	υ(C=N) imidazole	υ(SO_2)	υ(M-O)	υ(M-N)
HL_2	3419	1602	-------	-------	1143 1346		
$[Co(L_1\ L_2)H_2OCl]$	3400	1589	1413	1520	1143 1315	445	582
$[Ni(L_1\ L_2)H_2OCl]$	3361	1589	1417	1520	1141 1334	445	584
$[Cu(L_1\ L_2)H_2OCl]$	3373	1589	1419	1520	1151 1327	445	580
$[Zn(L_1\ L_2)H_2OCl]$	3400	1589	1429	1520	1143 1338	459	576
$[Cd(L_1\ L_2)H_2OCl]$	3415	1602	1419	1514	1141 1346	462	590
$[Hg(L_1\ L_2)H_2OCl]$	3400	1614	1417	1523	1147 1340	400	582
$[Fe(L_1\ L_2)Cl_2]$	------	1585	1417	1510	1143 1336	449	574
$[Au(L_1\ L_2)]Cl_2$	------	1616	1406	1510	1151 1334	462	511

5. Electronic Spectra

At room temperature, the spectra of electronic absorption of all the compounds were recorded by using solution of ethanol in the range 200-1100 nm. The spectral data of azo L_1, Schiff base HL_4 ligands and their metal complexes are summarized in Table (3). The spectral data of organic ligand (L_1) showed three charge transfer (C.T) bands at (208nm) (48076) cm^{-1} , (248 nm)(40322) cm^{-1} and (380nm)(26315) cm^{-1} attributed to $\pi\rightarrow\pi^*$, $\pi\rightarrow\pi^*$and $n\rightarrow\pi^*$ transition within the azo-ligand. The first band appeared at (208nm) can be ascribed to the ($\pi\rightarrow\pi^*$) transition of the phenyl rings while, the second band appeared at (248 nm) can be assigned to ($\pi\rightarrow\pi^*$) electronic transition due to electronic transition of the (-N=N-) group [29,30] The third band appeared in the visible region (380nm) can be assigned to $n\rightarrow\pi^*$ transition that including the whole electronic system of the azo dyes. The electronic spectrum of free Schiff base HL_2 ligand is characterized by two absorption bands in U.V-Visible. These bands are appearing at the positions of 290 nm (34482 cm^{-1}) and 358 nm (27932 cm^{-1}). The first band can be ascribed to the ($\pi\rightarrow\pi^*$) transition and second band can be attributed to a $n\rightarrow\pi^*$ transition [31], in addition to the presence of hetero atom carrying a lone pair of electrons in addition to intermolecular charge- transfer, this band showed at a red shift on coordination with a metal ions. The electronic spectrum of Co(II) complex displays three bands at 858nm (11655cm^{-1}) , 562 nm (17793 cm^{-1}), 477 nm (20964 cm^{-1}). These bands are assignable to $4T_1g$ (F)$\rightarrow{}^4T_2g$(F)= ν1 ${}^4T_1g(F)\rightarrow{}^4A_2g$ (F)=ν2, ${}^4T_1g(F)\rightarrow{}^4T_1g(p)$ = ν3 transitions respectively [32] .

The electronic spectrum of Ni(II) complex exhibited three absorption bands , at 802 nm (12468cm^{-1}), 700 nm (14285 cm^{-1}) and 574 nm (17421 cm^{-1}) and 467nm(21413cm^{-1}). These bands may be assigned to ${}^3A_2g\rightarrow{}^3T_2g$ (F) (v1) , ${}^3A_2g\rightarrow{}^3T_1g$(F) (v2) and ${}^3A_2g\rightarrow{}^3$T1g(p)(v3) and M→ L,CT transitions, respectively. The spectrum resembles those reported for octahedral complexes [33].

The electronic spectrum of the Cu(II) complex exhibited one absorption band at 476nm (21008cm^{-1}), this band is assignable to ${}^2Eg\rightarrow{}^2T_2g$ transitions. The broadness of the band may be due to Jahn-Teller distortion. All of these data suggested a distorted octahedral geometry around the Cu(II) ion.

The electronic spectrum of Au(III) complex displays one band at 554 nm (18050cm^{-1}) belong to ${}^1A_1g\rightarrow{}^1B_1g$

The electronic spectrum of Fe (III) complex exhibited five absorption bands, at 500 nm 20000 cm-1), 781nm (12804 cm-1) , 826 nm (12106 cm-1) ,1043nm (9587 cm-1) and 1065 nm (9389 cm-1) and 1096 (9124cm-1). These bands may be assigned to ${}^6A_1g\rightarrow{}^4T_1g$ (ν1), ${}^6A_1g\rightarrow{}^4T_2g$(ν2),^{6}A1g $\rightarrow{}^4$Eg,${}^4A_1g$ (ν3) ,and${}^6A_1g\rightarrow{}^4T_2g$(ν4), ${}^6A_1g\rightarrow{}^4$Eg(ν5) and ${}^6A_1g\rightarrow{}^4T_1g$ (ν6) transitions, respectively. The spectrum resemble those reported for octahedral complexes.

The electronic spectra of Zn (II), Cd (II) and Hg (II) complexes did not show any d→d transition because of saturation with electrons (d^{10}). The absorption bands at 485 nm

(20618cm^{-1}), 466 nm (21459cm^{-1}) and 558 nm (17921 cm^{-1}) may be assigned to a charge transfer transitions to Zn (II), Cd(II) and Hg (II) complexes respectively[35]. In Figure (4) the electronic spectra of the ligands and the complex of Cu (II) are shown. In Table (3)

Table (3): Magnetic moment, and electronic spectra of complexes

Compounds	λ (nm)	ύ (cm^{-1})	Transitions	Geometry	Hybridization	μ_{eff} (BM)
L_1	208 248 380	48076 40322 26315	π→π* π→π* n→π*	---------	----------	---------
HL_2	290 358	34482 27932	π →π* n →π*	----------	-----------	---------
$[Co(L_1L_2)\ H_2OCl]$	562 477	17793 20964	$^4T_1g(F)\rightarrow\ ^4T_2g(F)= v_1$ $^4T_1g(F)\rightarrow\ ^4T_1g(p) = v_3$	Octahedral	Sp^3d^2	4.11
$[Ni(L_1L_2)\ H_2OCl]$	802 700 574 467	12468 14285 17421 21413	$^3A_2g \rightarrow\ ^3T_2g_{(F)=}\ v_1$ $^3A_2g \rightarrow\ ^3T_1g_{(F)=}\ v_2$ $^3A_2g \rightarrow\ ^3T_1g_{(p)=}\ v_3$ M→L,CT	Octahedral	Sp^3d^2	3.42
$[Cu(L_1L_2)\ H_2OCl]$	476	21008	2Eg→2T2g	Octahedral	Sp^3d^2	1.73
$[Zn(L_1L_2)\ H_2OCl]$	485	20618	M→L,CT	Octahedral	Sp^3d^2	Dia
$[Cd(L_1L_2)\ H_2OCl]$	466	21459	M→L,CT	Octahedral	Sp^3d^2	Dia
$[Hg(L_1L_2)\ H_2OCl]$	558	17921	M→L,CT	Octahedral	Sp^3d^2	Dia

$[FeL_1L_2Cl_2]$	500 781 826 1043 1065 1096	20000 12804 12106 9587 9389 9124	$^6A_1g \rightarrow {}^4T1g = v_1$ $^6A_1g \rightarrow {}^4T2g = v_2$ $^6A_1g \rightarrow {}^4Eg, {}^4A_1g = v_3$ $^6A_1g \rightarrow {}^4T2g = v_4$ $^6A_1g \rightarrow {}^4Eg = v_5$ $^6A_1g \rightarrow {}^4T1g = v_6$	Octahedral	Sp^3d^2	para
$[Au\ L_1\ L_2]Cl_2$	554	18050	$^1A_1g \rightarrow {}^1B_1g$	square planer	dsp^2	Dia

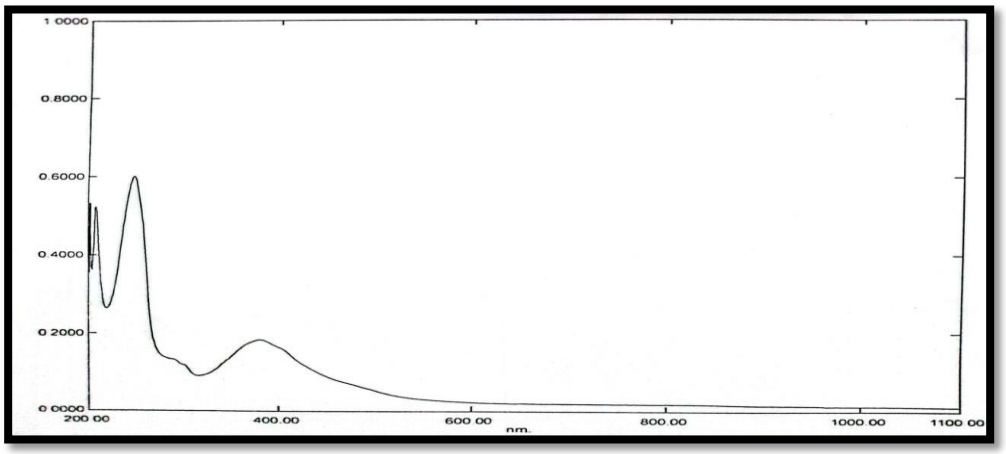

(a)

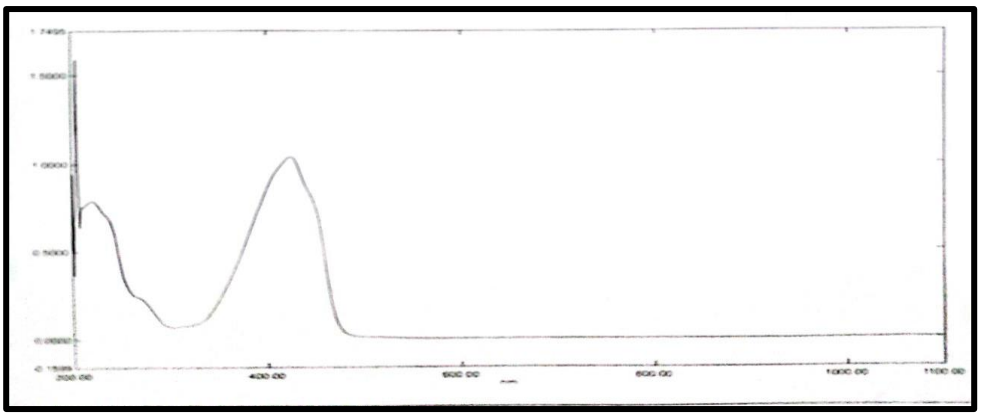

(b)

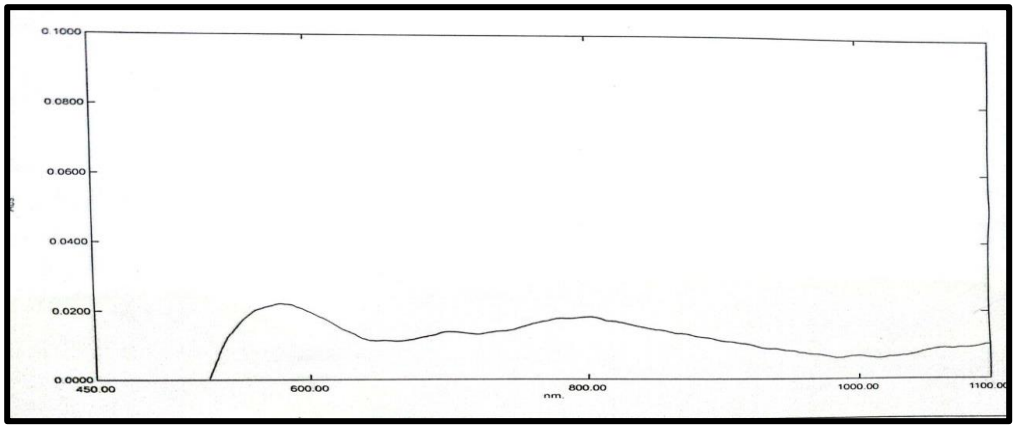

(c)

Figure (4) The spectra of electronic : (a) azo ligand & (b) Schiff base (c) mixed ligand complex of $[NiL_1L_2(H_2O)Cl]$

6. Measurement of conductivity

Molar conductance (Λm) measurements of the metal complexes were performed using ethanol as solvent at the concentration of 10^{-3} M in room temperature. In this work, all prepared chelate complexes exhibited the range values of conductivity between (**0.75-18.9**) $s.mol^{-1}.cm^2$ that non-electrolyte and non-conductive types ,While the molar conductance of Au(III) complex with mixed ligand is (80) $s.mol^{-1}.cm^2$ indicating the electrolytic nature (1:2) electrolyte of this complexes furthermore the chloride ions are located outside the coordination sphere [35-37]**.** It is possible to conclude structures of the complexes.

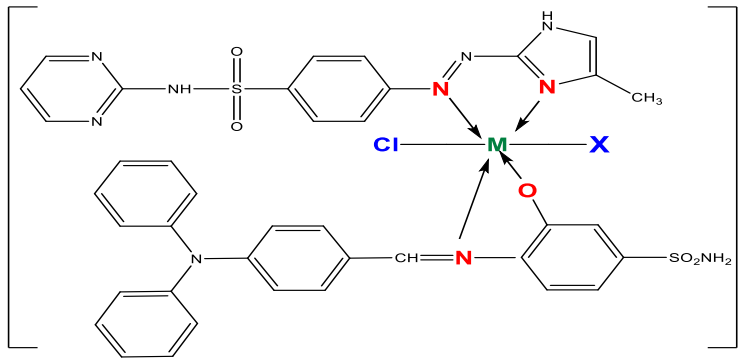

when M= Co(II) ,Ni(II) , Cu(II) ,Zn(II) ,Cd(II) ,Hg(II) , x=H2O
M=Fe , x=Cl

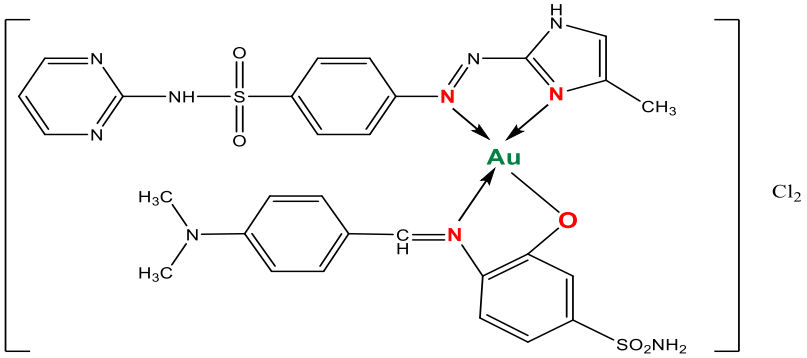

Scheme (4): the proposed structural formula of the complexes

7. *Antioxidant screening (DPPH radical scavenging activity)*

The scavenging activity results of some of synthetic compounds showed in table (4): From the results in table (4) and figure (5), the conc. (200) µg/mL is the most scavenging activity compared with other concentrations of synthesized compounds.

The DPPH is used in the laboratory and is widely used to evaluate the effectiveness of antioxidants. DPPH has absorption at 517 nm and disappears when DPPH is reduced to an antioxidant or becomes radical. The diamagnetic molecule is stable. As a result, the color changes from purple to yellow. This change in color is taken as an indicator of the ability y of hydrogen to donate to tested compounds.

Antioxidants can interact with DPPH and produce (1.1 - diphenyl - 2 - picryl – hydrazine). The limiting capabilities of the compounds examined were determined by their interaction with stable free-standing 1.1-di- vinyl-2-picryl-hydrazine (DPPH) in five different concentrations for 30 minutes

The highest scavenger activity observed in compound (HL_2), this is probably due to the presence of hydroxyl group. Mostly electron withdrawing substituent's deactivate aromatic ring and have no capability to bind the free radicals. The results of evaluating the activity of antioxidants showed that all the prepared compounds have antioxidant

properties when compared with standard antioxidants such as ascorbic acid as a reference in search of their antioxidant activity by the stable free radical method. [39-40]

Table 4: Scavenging activity of some synthetic compound

DPPH scavenging activity%						
Concentration	Ascorbic acid	L_1	HL_2	$[NiL_1L_2H2OCl]$	$[CuL_1L_2H_2OCl]$	$[AuL_1L_2]Cl_2$
50	65	69.3	83.9	65.5	62.7	68.9
100	73	69.7	92.7	69.5	66	75.9
150	85.3	69.8	93.4	70.1	67.7	78
200	98.2	71.7	94.9	77.1	68.6	78.7

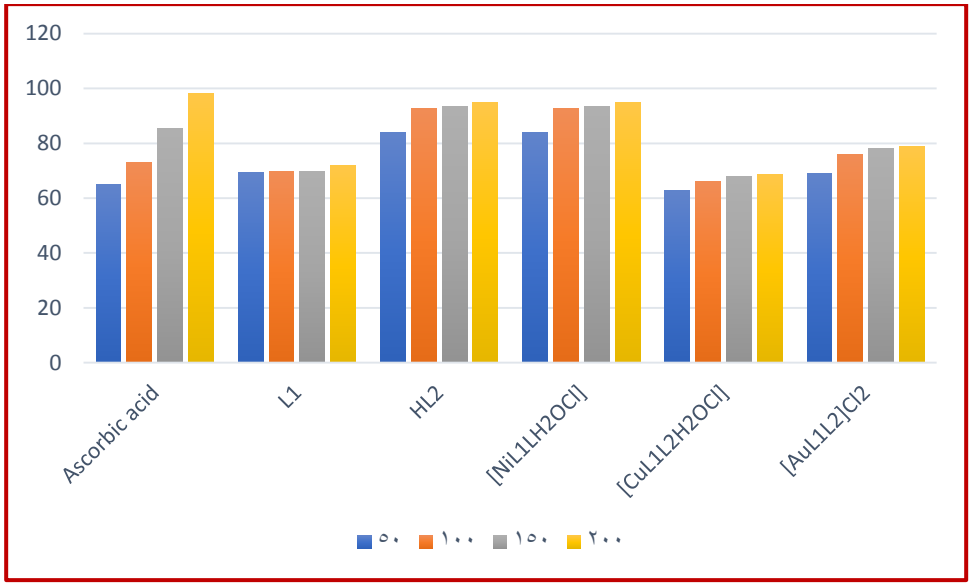

Figure (5): Scavenging activity of the compound using DPPH.

8. **Anticancer activity of gold complexes**

In vitro cytotoxic activity against breast cancer (MCF 7) cell line at different concentrations was evaluated and compared with the healthy cells The anticancer activities of the gold complexes were performed with different concentrations such as 6.25 µ g / ml ,12.25 µ g / ml , 25 µ g / ml , 50 µ g / ml , 100 µ g / ml. The anticancer activity of gold complexes against breast cancer (MCF 7) cell line increased while in the concentration of gold complexes (Fig. 6). Gold complexes exhibit good results when compare with the healthy cells. Previously the cytotoxic effect of gold nanoparticles is the result of active physicochemical interaction of gold atoms with the functional groups of intracellular proteins, as well as with the nitrogen bases and phosphate groups in DNA .

It was observed that half of the inhibitory concentration of cancer cells, IC50, was (145.27µg / ml), which is low compared to healthy cells, where it was (192.21µg / ml), and this is a good result. That is, the gold nanocomplex kills breast cancer cells with high efficiency and has no effect on healthy cells. This is a very important result in the use of a complex of gold as a highly selective treatment for the treatment of breast cancer.

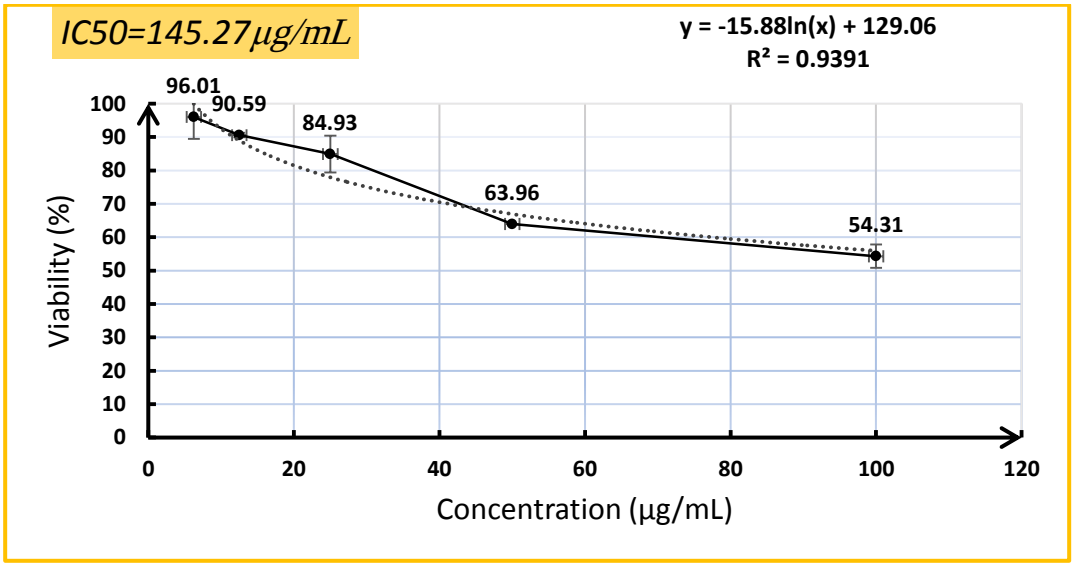

(a)

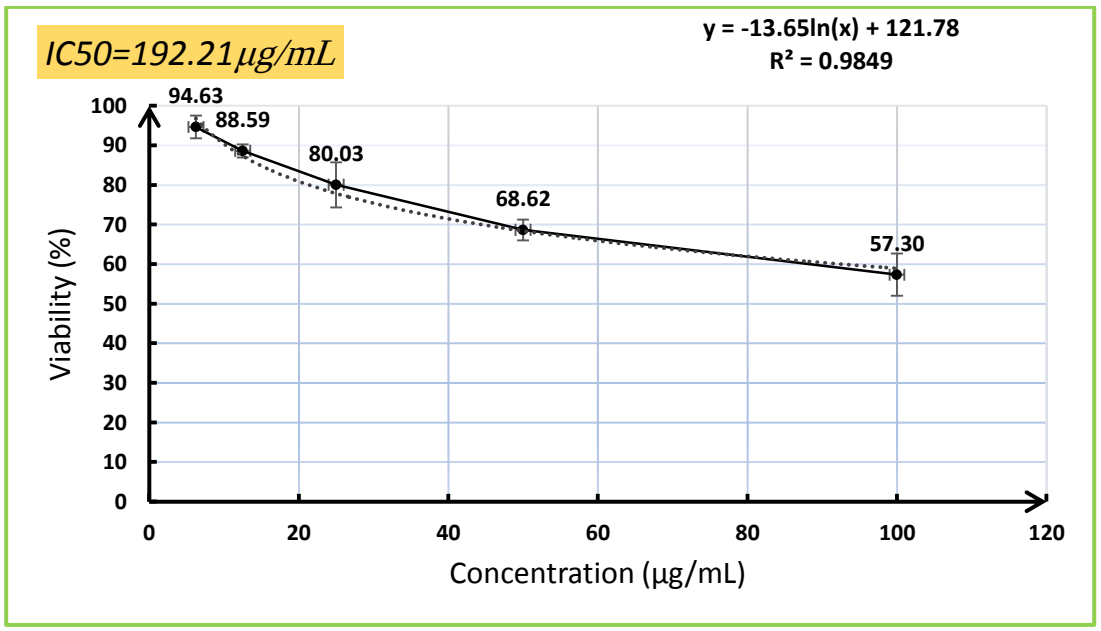

(b)

Figure (6): Percentage of inhibition in cells of (a) MCF-7 breast cancer line cell against the concentration of complex [Au L_1L_2]Cl_2 (b) normal line cell against the concentration of complex [Au L_1L_2]Cl_2

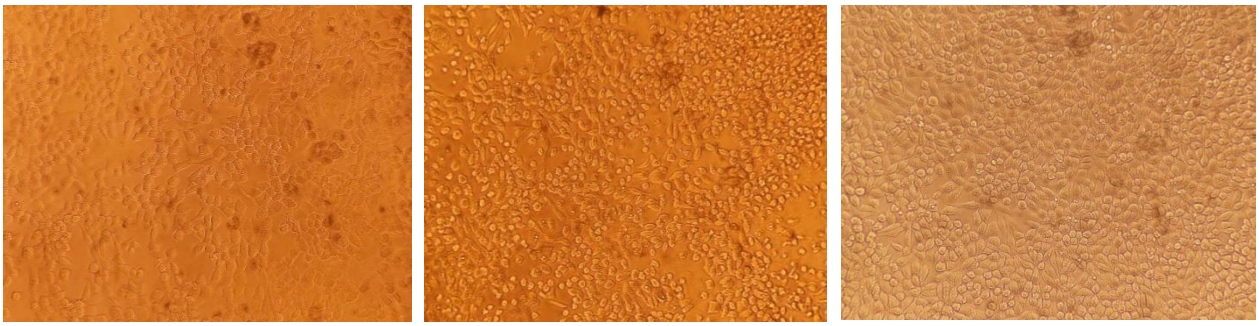

(a)

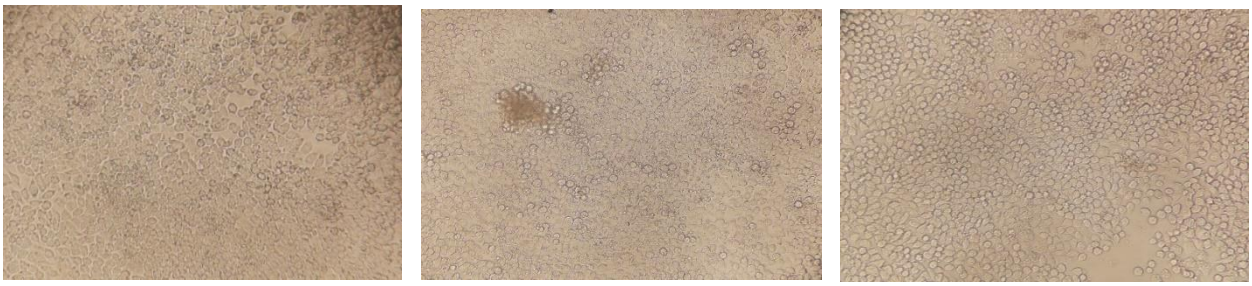

(b)

Figure (7):(a) Cancer cells treated with compound [AuL_1L_2]Cl_2 at different concentration after adding MTT (b)Normal cells treated with compound [AuL_1L_2]Cl_2 at different concentration after adding MTT

References:

1. Brand, A., and Uhl, W. (2019). Sterically Constrained Bicyclic Phosphines: A Class of Fascinating Compounds Suitable for Application in Small Molecule Activation and Coordination Chemistry. Chemistry–A European Journal, 25(6), 1391-1404.
2. Cai, H., Huang, Y. L., and Li, D. (2019). Biological metal–organic frameworks: structures, host–guest chemistry and bio-applications. Coordination Chemistry Reviews, 378, 207-221.

3. Radisavljević, S., Petrović, B. (2020). Gold (III) Complexes: An Overview on Their Kinetics, Interactions With DNA/BSA, Cytotoxic Activity, and Computational Calculations. Frontiers in Chemistry, 8, 379.
4. Yeo, C. I., Ooi, K. K., & Tiekink, E. R. (2018). Gold-based medicine: a paradigm shift in anti-cancer therapy?. Molecules, 23(6), 1410.
5.Wen, X., Liu, S., Sheng, J., & Cui, M. (2020). Recent advances in the contribution of noncoding RNAs to cisplatin resistance in cervical cancer. PeerJ, 8, e9234.
6. Buldurun, K., Turan, N., Savcı, A., & Çolak, N. (2019). Synthesis, structural characterization and Biological activities of metal (II) complexes with Schiff bases derived from 5-bromosalicylaldehyde: Ru (II) complexes transfer hydrogenation. Journal of Saudi Chemical Society, 23(2), 205-214.
7. Bagdatli, E., Altuntas, E., & Sayin, U. (20 .(17Synthesis and structural characterization of new oxovanadium (IV) complexes derived from azo-5-pyrazolone with prospective medical importance. Journal of Molecular Structure, 1127, 653-661.
8. Abdel-Mottaleb, M. S., & Ismail, E. H. (2019). Transition Metal Complexes of Mixed Bioligands: Synthesis, Characterization, DFT Modeling, and Applications. Journal of Chemistry, 2019.
9. Aly, S. A., & Fathalla, S. K. (2020). Preparation, characterization of some transition metal complexes of hydrazone derivatives and their antibacterial and antioxidant activities. Arabian Journal of Chemistry, 13(2), 3735-3750.
10. Mirzaee, E., Zamani, H. A., & Mohammadhosseini, M. (2019). Construction of a New Selective and Sensitive Nd3+ ion-selective Electrode Based on 1-nitroso-2-naphtol as a Neutral Ion Carrier. Int. J. Electrochem. Sci, 14, 693-704.
11. Devic, T., Lestriez, B., & Roué, L. (2019). Silicon electrodes for Li-ion batteries. Addressing the challenges through coordination chemistry. ACS Energy Letters, 4(2), 5.557-50
12. Al-Zaidi, B. H., Hasson, M. M., & Ismail, A. H. (2019). New complexes of chelating Schiff base: Synthesis, spectral investigation, antimicrobial, and thermal behavior studies. J. Appl. Pharm. Scie, 9, 045-057.
13. Marzec, A., Szadkowski, B., Rogowski, J., Maniukiewicz, W., Kozanecki, M., Moszyński, D., & Zaborski, M. (2019). Characterization and properties of new color-tunable hybrid pigments based on layered double hydroxides (LDH) and 1, 2-dihydroxyanthraquinone dye. Journal of Industrial and Engineering Chemistry, 70, 427-438.

14. Al-Adilee, K. J. and Haitham K.D. ,(2018). Eurasian Journal of Analytical Chemistry, 13(5), 2-17.
15. Nada H. H. and Raheem T. M. (2019). International Journal of Pharmaceutical Research , 11(1)
16. B.shunlichiro and D.carter and Q.fernand; (1967) Chem.Comun, 1301.
17. Teshima, N., Murakami, H., & Sakai, T. (2020). Development of Testing Methods for Water Quality by Flow Analysis. Bunseki Kagaku, 69(6), 257-269.
18. Habiban, A. M., Mahmoud, W. A., & Kareem, T. A. (2015). Preparation and Characterization of Metal Complexes with Heterocyclic Azo Ligand (4-SuBAI). Baghdad Science Journal, 12(3), 503-515.
19. Zainab. A. A. and Abdullah. M. A. (2015). Preparation and Characterization of Some New Mixed Ligand with Complexes of Copper(II). International Journal of Novel Research in Interdisciplinary Studies. 1(2), 5-13.
20. Shih MH, Ke FY. Synthesis and evaluation of antioxidant activity of sydnonyl substituted thiazolidinone and thiazoline derivatives. Bioorg Med Chem. 2004;12:4633e4643.
21. Daisuke N, Yuko W, Yasuhiro F, 2014 A Novel Square-Planar Ni(II) Complex with an Amino— Carboxamido-Dithiolato-Type Ligand as an Active-Site Model of NiSOD *Inorg. Chem*., **53** 6512–6523.
22. Layla A M, Mithaq S M, Muna A H, 2020 Formation, Characterization, Basic Studies and Biological Effect of Mixed Ligand Complexes of Cu-ion and Ni-ion Derived from Azo Compounds, Schiff bases and (1,10, phen) *International Journal of Pharmaceutical Research*, **12** 1.238.
23. Waleed A, Amir M and Nadia H 2017, Preparation and Characterization of New Azo LigandN-[(1-(4-(4,5-Dimethyl-1h-Imidazol-2-Yl) Diazenyl) Phenyl-3-(Trifluoromethyl)] Aniline With Some Metal Complexes, *Acta Chimica PharmaceuticaIndica*, 1 35
24. Ragip A, Nevin T, Kenan B and Hanifi K, Spectral, Thermal and Antimicrobial properties of Novel Mixed Ligand -Metal Complexes Derived from Saccharinate Complexes and Azo Dye Ligand, International Journal Pharmagology, 2018; 8(3): 1811-1820.
25. Hasan A, Wasan MA, Riyadh MA and Enaam IY, Synthesis, characterization of Some Mixed-Ligand Complexes Containing Azo Dye and 1,10- phenanthroline with CoII, ZnII, CdII and HgII Ions, Ibn AL-Haitham Jour. for Pure α Appl. Sci., 2015; 28(3): 156-76.
26. Israa W, Zahraa Y and Mbarik MH, Synthesis, characterization, and Biological Efficacy on new mixed ligand complexes based from Azo dye of 8- hydroxy quinoline as a primary ligand and Imidazole as a secondary ligand with some of

transition metal ions, Journal of Pharmaceutical sciences and Research., 2018; 10(12): 3074-3084.
27. Nagham MA, Synthesis and Chemical Identification of Macro Compounds of (Thiazol and Imidazol), Research J. Pharm. and Tech., 2015; 8(1): 78-84.
28 D. P. Patel, S. P. Prajapati, A. K. Rana and P. S. Patel, Der Che. Sci., 3(2), 491-496 (2012).
29. Mohamad M, 2013 Some transition metal complexes with new Schiff base ligand hexa dentate, Actachimica. Pharm. Indica., 3 140–148.
30. Hiroki S, Izumi B, Tomoyuki H, Takashiro A, Rakesh P. 2018 Optical properties of chiral Schiff base MnII,CoII: J.Indian Chem.Soc. 95

31. Al-Salami B., Gata R. and Asker K. , synthesis spectral, thermal stability and Bacterial Activity of Schiff Base Derived from Selective Amino Acid and Their complexes. Pelagia Research libray, , 8(3): 4 – 12. (2017).
32. Siham S. , Abbas H. , Preparation and Biological Activities of New Heterocyclic Azo Ligand and Some of Its Chelate Complexes , Nano Biomed. 10(1): 46-55 (2018).

33. Penicillin: Characterization, Molecular Modeling, and Antibacterial Activity Study ., Bioinorganic Chemistry and Applications 1-13 (2017).
34. Mohamad M. , some transition metal complexes with new Schiff base ligand hexa dentate. Acta chimica. Pharm. Indica, , 3(2): 140 – 148 (2013) .
35. Layla A M, Raheem T M, Abid A, 2020 Synthesis, identification and structural of some transition metal complexes with New heterocyclic azo-schiff base ligand derived from 4-amino antipyrine International Journal of Pharmaceutical Research , 12 4
36. Penicillin: Characterization, Molecular Modeling, and Antibacterial Activity Study, Bioinorganic Chemistry and Applications, 2017, 1-13 .
37. Alaa J, 2018 Synthesis and Characterization of Complexes Ions Co (II) and Ni(II) with new Ligand IJARIIE 4
38. Penicillin: Characterization, Molecular Modeling, and Antibacterial Activity Study ., Bioinorganic Chemistry and Applications 1-13 (2017).
39. Bagheri, M., Validi, M., Gholipour, A., Makvandi, P., & Sharifi, E. (2022). Chitosan nanofiber biocomposites for potential wound healing applications: Antioxidant activity with synergic antibacterial effect. Bioengineering & translational medicine, 7(1), 10254.
40. Shen, N., Wang, T., Gan, Q., Liu, S., Wang, L., & Jin, B. (2022). Plant flavonoids: Classification, distribution, biosynthesis, and antioxidant activity. Food Chemistry, 383, 132531.